JOURNAL OF GEOPHYSICAL RESEARCH, VOL. 104, NO. A9, PAGES 19,843–19,849, SEPTEMBER 1, 1999

Solar wind electrons: Parametric constraints

S. Peter Gary, Elena Neagu, and Ruth M. Skoug
Los Alamos National Laboratory, Los Alamos, New Mexico

Bruce E. Goldstein
Jet Propulsion Laboratory, Pasadena, California

Abstract. Solar wind electrons are often observed to consist of two distinguishable components, a thermal, more dense core and a suprathermal, less dense halo. In this core/halo model linear Vlasov theory for the whistler heat flux instability predicts dimensionless heat flux thresholds which decrease as the electron core beta, $\tilde{\beta}_{\|c}$, increases. It has been proposed that this theoretical threshold corresponds to an observable upper bound on the electron heat flux. Linear theory also predicts that there is a critical value of $\tilde{\beta}_{\|c}$ below which the whistler heat flux instability does not have appreciable growth in the solar wind; there is another suggestion that this corresponds to an observable lower bound on $\tilde{\beta}_{\|c}$. These two proposals are examined by comparison of linear theory and data from the initial in-ecliptic phase of the Ulysses mission. The instability threshold does provide a statistical constraint on observed solar wind heat fluxes, and the critical $\tilde{\beta}_{\|c}$ of theory is not inconsistent with a statistical lower bound on the observations of that parameter.

1. Introduction

A primary goal of space plasma physics theory should be to provide descriptions of fundamental small-scale plasma processes that not only explain existing observations, but also predict the results of future measurements. These descriptions should be both quantitative and concise, not only to facilitate their comparisons against observations but also to enable their use in large-scale models of space and astrophysical plasmas. The research described here is directed toward this goal, addressing basic issues of electron heating and thermal transport in the solar wind and providing simple, quantitative expressions for constraints on electron temperatures and heat fluxes imposed by small-scale enhanced field fluctuations from the whistler heat flux instability.

Solar wind electron velocity distributions are often observed to consist of two distinguishable components, a thermal, more dense core (denoted by subscript c) and a suprathermal, less dense halo (subscript h) [*Feldman et al.*, 1975; *Marsch*, 1991]. The relative drift of these two components corresponds to an electron heat flux $\mathbf{q}_e$ directed along the local background magnetic field $\mathbf{B}_o$. This $\mathbf{q}_e$ is a fundamental property of the solar wind, constituting an important channel of energy flow from the hot solar source to the cold outer heliosphere [*Feldman et al.*, 1998].

However, this energy flow, and the associated issue of electron core heating, are not well understood. There are several analyses of global scaling of average electron properties with R, the distance from the Sun in astronomical units. Observations from both the Helios spacecraft for low-speed streams and sector boundaries between 0.3 and 1 AU [*Pilipp et al.*, 1990] and from the Ulysses spacecraft in the ecliptic plane between 1 and 5 AU [*Scime et al.*, 1994b] show $q_e \sim R^{-3}$. In contrast free expansion along the local magnetic field predicts $q_e \sim R^{-2}$ at small R and $\sim R^{-1}$ for large R [*Scime et al.*, 1994b]. Furthermore, the average electron core temperature in the ecliptic plane is observed from Ulysses to decrease as $R^{-0.9}$ [*Scime et al.*, 1994b; *Phillips et al.*, 1995] and even more slowly from Helios ($T_c \sim R^{-\alpha_c}$, where α_c ranges from 0.48 to 0.84 [*Pilipp et al.*, 1990]), in contrast to the $R^{-4/3}$ scaling predicted by adiabatic fluid theory as well as by some kinetic models of solar wind electrons [*Meyer-Vernet and Issautier*, 1998]. Analysis of local, statistical data sets also has yielded unexplained results, including the *Newbury et al.* [1998] observation that the solar wind electron temperature has a lower bound which is a function of the proton temperature.

The strong decrease of q_e with R, representing a heat flux reduction beyond the free streaming model, may or may not be related to the relatively weak decrease with R of T_c, which implies electron core heating in addition to adiabatic cooling. Heat flux instabilities have the potential to contribute to both nonideal processes. In particular there is both local [*Feldman et al.*, 1976a, 1976b] and global [*Gary et al.*, 1994; *Scime et al.*, 1994b] evidence that the whistler heat flux instability plays a role in the reduction of q_e in the solar wind. Core electrons, however, are weakly resonant with the whistler heat flux instability and may not be strongly heated by enhanced fluctuations from this growing mode. Other growing modes, such as the Alfvén heat flux instability, have stronger core resonances and may provide the necessary heating, although their role in limiting the heat flux is less clear.

If the anisotropy of a species velocity distribution becomes sufficiently large in a relatively collisionless, relatively

Paper number 1999JA900244.
0148-0227/99/1999JA900244$09.00

homogeneous plasma, one or more instabilities will be excited. The enhanced field fluctuations which arise lead to wave-particle interactions which reduce the anisotropy, constraining it from exceeding some value which may correspond to an instability threshold condition predicted by linear Vlasov theory. A well-established example of such a constraint is the upper bound imposed upon the hot proton temperature anisotropy by the electromagnetic proton anisotropy instability in a plasma with a bi-Maxwellian hot proton distribution and $T_{\perp p}/T_{\|p} > 1$. (See the appendix for the definitions of these and other symbols used here.) For this instability, there is good agreement among linear theory, which predicts a threshold condition, hybrid simulations, which demonstrate that this threshold corresponds to an anisotropy constraint, and spacecraft observations, which confirm that this bound applies statistically in both the outer magnetosphere [*Gary et al.*, 1995] and the magnetosheath [*Gary et al.*, 1997, and references therein].

In the analogous case of a single bi-Maxwellian electron distribution with $T_{\perp e}/T_{\|e} > 1$, the whistler anisotropy instability is excited with linear theory properties as summarized by *Gary and Wang* [1996]. The linear theory threshold of this instability takes the form

$$\frac{T_{\perp e}}{T_{\|e}} - 1 = \frac{S_e}{\beta_{\|e}^{\alpha_e}} , \qquad (1)$$

where S_e and α_e are fitting parameters and $\alpha_e \simeq 0.5$. *Gary and Wang* [1996] used computer simulations to show that the electron temperature anisotropy is indeed constrained by this condition. However, unlike the proton temperature anisotropy case, the electron temperature anisotropy upper bound has not yet been verified by observations. Solar wind conditions are not appropriate to test this constraint because the typical electron component anisotropy is $T_\perp < T_\|$. However, there is another electron anisotropy which is more likely to drive instabilities and may be used for an observational test of the general concept of anisotropy constraints in the solar wind. That anisotropy is the electron heat flux.

In the low latitude, low-speed wind at $v_{sw} \lesssim 500$ km/s, the velocity distributions of both halo and core may approximately be represented as bi-Maxwellians with relative drift velocity $\mathbf{v}_o$ parallel to $\mathbf{B}_o$ [*Feldman et al.*, 1975; *Maksimovic et al.*, 1997]. For our theory we assume such a model and further assume the conditions of quasineutrality ($\Sigma_j e_j n_j = 0$) and zero current ($\Sigma_j e_j n_j \mathbf{v}_{oj} = 0$) where the summation is over all plasma species. Also assuming that the solar wind ions consist only of a single Maxwellian proton component, then the properties of instabilities driven by electron anisotropies are determined by the following dimensionless parameters: n_h/n_i, v_o/v_A, $T_{\|h}/T_{\|c}$, $T_{\perp c}/T_{\|c}$, $T_{\perp h}/T_{\|h}$, $T_{\|c}/T_p$, and $\tilde{\beta}_{\|c}$. (The halo/core relative drift may also be characterized in terms of the dimensionless heat flux $q_e/q_{\max}$.) The parameter v_A/c is always much less than unity in the solar wind and its variations do not significantly change the properties of the instabilities considered here.

For a broad range of parameters in this solar wind electron model, the core/halo instability of lowest threshold is the whistler heat flux instability [*Gary et al.*, 1975a, b; *Abraham-Shrauner and Feldman*, 1977; *Gary*, 1978], and indeed there is substantial observational evidence of enhanced whistler-like fluctuations in the solar wind [*Lengyel-Frey et al.*, 1996; *Lin et al.*, 1998]. *Gary et al.* [1994] showed that, if $T_{\perp c}/T_{\|c} = T_{\perp h}/T_{\|h} = 1$, this instability threshold assumes the form

$$\frac{q_e}{q_{\max}} = \frac{S_q}{\tilde{\beta}_{\|c}^{\alpha_q}} , \qquad (2)$$

where S_q and α_q are fitting parameters and $\alpha_q \simeq 0.85$ on the domain $0.25 \leq \tilde{\beta}_{\|c} \leq 4.0$. If the core and halo bear temperature anisotropies, this threshold condition involves additional terms proportional to $T_{\perp c}/T_{\|c} - 1$ and $T_{\perp h}/T_{\|h} - 1$. Further, *Gary et al.* [1994] proposed that the whistler instability threshold should correspond to an observable upper bound on the solar wind heat flux and presented some evidence in support of this.

Gary et al. [1998] showed that the whistler heat flux instability does not have appreciable growth below some limiting value of $\tilde{\beta}_{\|c} \ll 1$. Other modes, such as the Alfvén heat flux instability, can grow at lower values of $\tilde{\beta}_{\|c}$, as illustrated, for example, in Figure 3 of *Gary et al.* [1998]. Thus there is a critical value of this parameter which separates the parametric domain on which the whistler instability is most likely to grow from the domain on which other heat flux instabilities are likely to dominate. Furthermore, *Gary et al.* [1998] hypothesized that the whistler instability does not heat the core, but that other heat flux instabilities may heat core electrons, implying that the critical value of $\tilde{\beta}_{\|c}$ corresponds to a lower bound on that parameter. This constraint is fundamentally different from the anisotropy bounds represented by the above equations; it concerns a parameter which does not correspond to an anisotropy, and it is derived from the transition from one unstable mode to another, rather than from the transition from stability to instability of a single mode.

There are three major parts to this manuscript. In the first part, consisting of Sections 2 and 3, we present results of statistical analyses of electron dimensionless parameters observed from the in-ecliptic phase of the Ulysses mission as functions of $\tilde{\beta}_{\|c}$. This extends previous such work which derived scaling relations for the average values of solar wind dimensionless parameters only as functions of R. In the second part of the manuscript, Section 4, these scalings are used in linear Vlasov theory to derive average threshold conditions for the whistler heat flux instability as a function of $\tilde{\beta}_{\|c}$, and to obtain a theoretical scaling for the critical value of $\tilde{\beta}_{\|c}$ as a function of R. Finally, in Section 5 these theoretical results are compared against Ulysses data to test whether they constitute observable statistical constraints on solar wind electron parameters.

2. Data Analysis: Recent Ulysses Results

Our data analysis used Ulysses observations made with the Los Alamos solar wind ion and electron Solar Wind Observations Over the Poles of the Sun (SWOOPS) spectrometers [*Bame et al.*, 1992]. We used parameters obtained from the most recent data reduction procedures, including an improved technique for taking account of spacecraft charging effects [*Scime et al.*, 1994a] and an April 1999 correction to a minor error in the algorithm which computes

electron temperature anisotropies. *Scime et al.* [1994b] examined scalings of SWOOPS observations in the ecliptic plane from 1.2 to 5.4 AU; they found $n_e = 5.2R^{-2.0}$ cm^{-3}, $T_c = 1.3 \times 10^5 R^{-0.85}$ K, $T_h = 9.2 \times 10^5 R^{-0.38}$ K, and $q_e = 10.5R^{-3.0}\mu$W/m^2. In addition, the R dependences of several dimensionless parameters reported by *Gary et al.* [1994] are stated in the middle column of Table 1. *Phillips et al.* [1995] presented results from the initial out-of-ecliptic phase of the Ulysses mission from February 1992 through December 1993; they found little change with heliographic latitude in the means of either the core temperature (at $T_c \simeq 3.0 \times 10^4$ K) or the core anisotropy (at $T_{\perp c}/T_{\|c} \simeq 0.82$).

3. Data Analysis: Scaling Relations

This section describes our statistical analysis of Ulysses electron data. Our concern, which has not been addressed previously, is the variation of dimensionless electron parameters with $\tilde{\beta}_{\|c}$ within relatively narrow domains of R. The $\tilde{\beta}_{\|c}$ is one of the most fundamental parameters determining electromagnetic instability properties in both linear theory [*Gary et al.*, 1994] and simulations [*Gary and Wang*, 1996]. This parameter can vary by two orders of magnitude in a solar wind domain, so it is important to determine how other dimensionless parameters vary with $\tilde{\beta}_{\|c}$ as well as with R in order to more fully understand how plasma instabilities respond to changes in solar wind conditions.

We used Ulysses data from the high resolution electron database described by *Scime et al.* [1994b]. From the initial in-ecliptic phase of the mission we analyzed core and halo moments derived by integration of the three-dimensional measurements which have been rotated into a coordinate system with one axis parallel to $\mathbf{B}_o$. We sorted data into nine radial bins, corresponding to $1.6 \le R < 2.0$, $2.0 \le R < 2.4$, ... $4.8 \le R < 5.2$. We considered only data from the low-speed wind ($v_{sw} \le 500$ km/s); in the high-speed wind electron "strahl" are more frequently present [*Marsch*, 1991; *Fitzenreiter et al.*, 1998] and the suprathermal electrons are not well represented as a bi-Maxwellian halo. In addition, we considered only data which met the following conditions: (1) $|n_e - n_i| \le 0.5n_i$ where $n_i = n_p + 2n_\alpha$ and $n_e = n_c + n_h$, (2) $n_h < 0.30n_i$, and (3) the values of $\log(n_h/n_i)$ and $\log(\tilde{\beta}_{\|c})$ fell within 3σ of the mean values in each bin. Each of these three conditions was imposed to exclude unphysical outlier points in the electron data set which are relatively rare yet which can cause severe skewing of average values. We also excluded data when the analysis algorithm failed to properly compute a core, halo, or total ion density. On the other hand, we did not exclude data associated with coronal mass ejections or shocks.

Figure 1 illustrates five dimensionless variables as functions of $\tilde{\beta}_{\|c}$ for Ulysses observations at $2.0 \le R < 2.4$, along with the least squares fits to the form $S_\Psi/\tilde{\beta}_{\|c}^{\alpha_\Psi}$. The results here are characteristic of most radial bins; the α_Ψ for the core and halo temperature anisotropies as well as for $T_{\|h}/T_{\|c}$ are typically close to zero so that the average values of these three dimensionless quantities are usually weak functions of $\tilde{\beta}_{\|c}$. The parameter with the strongest $\tilde{\beta}_{\|c}$ dependence is $q_e/q_{\max}$ with a mean value which in this radial bin varies as $\tilde{\beta}_{\|c}^{-0.34}$.

By fitting the median values of the dimensionless parameters in successive radial bins as power laws with distance from the Sun, we obtain expressions for these quantities which are functions of R alone. These results are stated in the right column of Table 1 and for the most part agree with the R dependences reported by *Gary et al.* [1994]. In contrast to some dimensional parameters such as the density and the heat flux which decrease rapidly with distance from the Sun, all the dimensionless parameters described here are comparatively weak functions of R.

Table 1. Scalings for Dimensionless Parameters: Ulysses Observations

Parameter	*Scime et al.* [1994b] and *Gary et al.* [1994]	This Work: Medians
n_h/n_e	$0.06R^{-0.25}$	
n_h/n_i		$0.067R^{-0.24}$
$T_{\perp c}/T_{\|c}$	0.83	$1.01R^{-0.10}$
$T_{\perp h}/T_{\|h}$	0.74	$0.75R^{0.045}$
$T_{\|h}/T_{\|c}$	$7.5R^{0.40}$	$7.9R^{0.30}$
$q_e/q_{\max}$	$0.46R^{-0.19}$	$0.61R^{-0.023}$

4. Linear Theory: Threshold Conditions

In this section we present results from linear Vlasov dispersion theory analyses of the whistler heat flux instability. This mode has maximum growth rate at $\mathbf{k} \times \mathbf{B}_o = 0$, so we used the dispersion equation corresponding to that condition and dimensionless parameters from Table 1. The linear theory properties of this mode are independent of $T_{\|c}/T_p$ for a broad domain of solar wind conditions and $\tilde{\beta}_{\|c} \lesssim 2.5$, so the choice of $T_{\|c}/T_p$ (which we here take to be 2.0) does not significantly affect the thresholds computed here for most values of $\tilde{\beta}_{\|c}$.

To determine the local (that is, the $\tilde{\beta}_{\|c}$-dependent) average threshold conditions for the whistler heat flux instability, we used the $\tilde{\beta}_{\|c}$-dependent expressions for the mean values of $T_{\perp c}/T_{\|c}$, $T_{\perp h}/T_{\|h}$, $T_{\|h}/T_{\|c}$, and n_h/n_i for each of the nine radial bins. We then varied v_o/v_A (or equivalently $q_e/q_{\max}$) to calculate the $\gamma_m/\Omega_p = 0.01$ average threshold condition for the whistler heat flux instability in each bin over $0.10 \le \tilde{\beta}_{\|c} \le 5.0$, obtaining a threshold condition of the form of (2). (A sample computation confirmed the indication of Figure 2 of *Gary et al.* [1998] that there is no significant change in the instability threshold at $\gamma_m/\Omega_p < 0.01$.) Although neither fitting parameter showed a clear trend with R, the median values yielded

$$S_q = 1.0\ ,\ \alpha_q = 0.8 \tag{3}$$

over $0.10 \le \tilde{\beta}_{\|c} \le 5.0$. This empirical result is similar to those from two different theoretical determinations: the linear theory threshold calculations of the whistler heat flux instability of *Gary et al.* [1994] and the quasilinear determination of a heat flux inhibition due to this same instability by *Pistinner and Eichler* [1998]. It is also in relatively

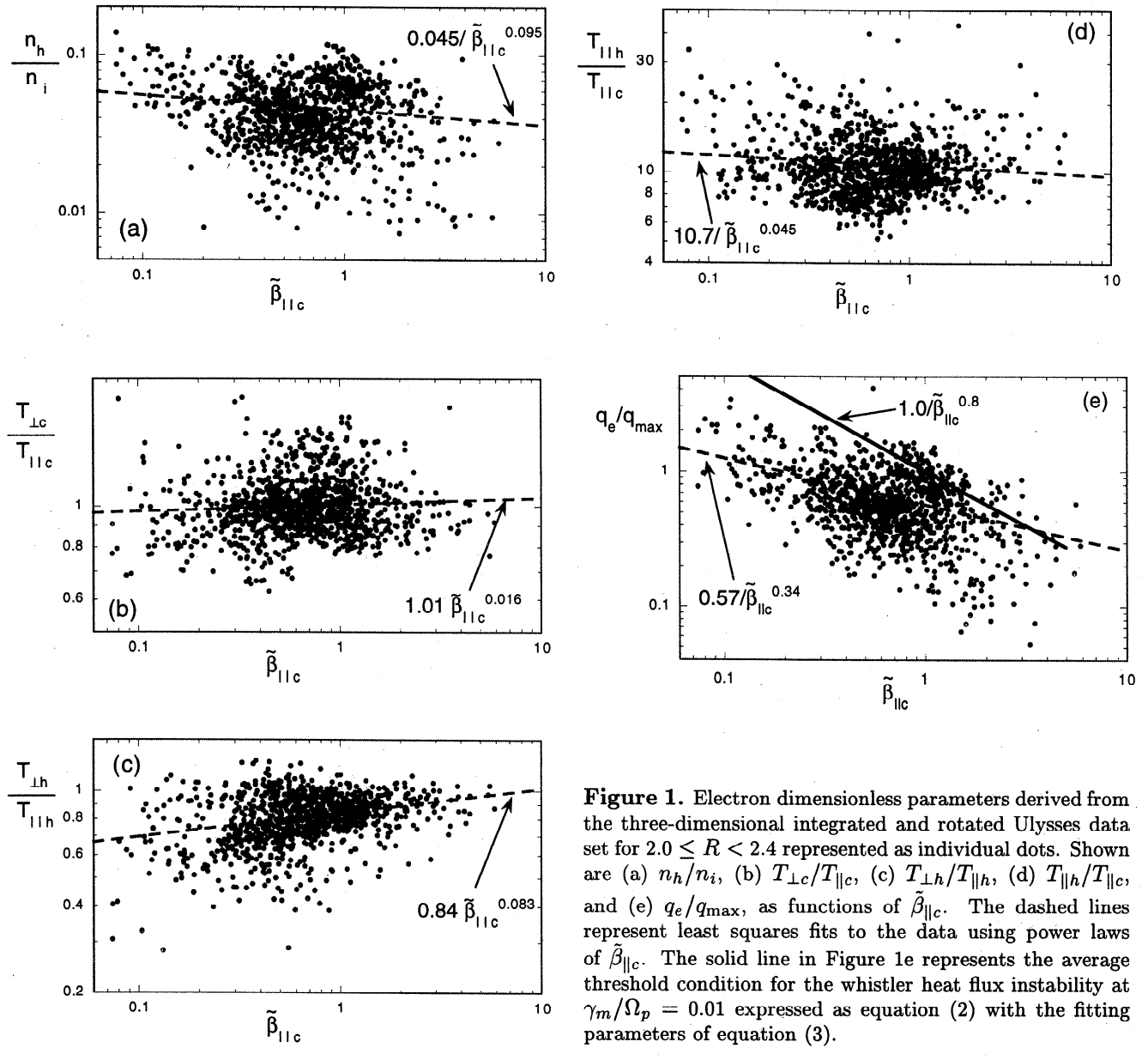

Figure 1. Electron dimensionless parameters derived from the three-dimensional integrated and rotated Ulysses data set for $2.0 \leq R < 2.4$ represented as individual dots. Shown are (a) n_h/n_i, (b) $T_{\perp c}/T_{\|c}$, (c) $T_{\perp h}/T_{\|h}$, (d) $T_{\|h}/T_{\|c}$, and (e) $q_e/q_{\max}$, as functions of $\tilde{\beta}_{\|c}$. The dashed lines represent least squares fits to the data using power laws of $\tilde{\beta}_{\|c}$. The solid line in Figure 1e represents the average threshold condition for the whistler heat flux instability at $\gamma_m/\Omega_p = 0.01$ expressed as equation (2) with the fitting parameters of equation (3).

good agreement with the empirical upper bound of (2) with $S_q = 0.85$ and $\alpha_q = 0.82$ obtained by *Gary et al.* [1999] from Ulysses observations during February and March 1995.

We next examined the critical value of $\tilde{\beta}_{\|c}$ which we define as the value below which the whistler heat flux instability can grow no faster than a certain γ_m/Ω_p. To determine how this critical value scales with R, we once again used the $\tilde{\beta}_{\|c}$-dependent expressions for the mean values of $T_{\perp c}/T_{\|c}$, $T_{\perp h}/T_{\|h}$, $T_{\|h}/T_{\|c}$, and n_h/n_i for each of the nine radial bins as the basis of our calculations. We then varied v_o/v_A and $\tilde{\beta}_{\|c}$ to construct families of curves at $\gamma_m/\Omega_p = 0.10$ similar to the whistler curve of Figure 3 of *Gary et al.* [1998]. Each curve corresponding to a different radial bin yields a corresponding critical value of $\tilde{\beta}_{\|c}$; fitting the results to a power law in R, we obtained

$$\tilde{\beta}_{\|c} \simeq \frac{0.40}{R^{1.3}} \tag{4}$$

over the domain $1.8 \leq R \leq 5.0$. In the next section we return to the analysis of Ulysses electron data and compare the constraints derived above against observations.

5. Applications: Parametric Constraints

Figure 1e illustrates a comparison of observations and linear theory. Here the solid line is the average threshold of the whistler heat flux instability (equation (2) with fitting parameters from equation (3)). In this figure less than 9% of the data (94 points out of 1139 total) lie above the line. In contrast, a larger number of the points cluster relatively close to, but below, the average threshold, indicating that this condition represents an upper bound on the dimensionless heat flux. Plots of the same quantities for the eight other radial bins show qualitatively similar results. Figures 2a and 2b illustrate this for two other radial bins; in each case less than 2% of the data lie above the threshold line and a much larger number of points cluster just below this line

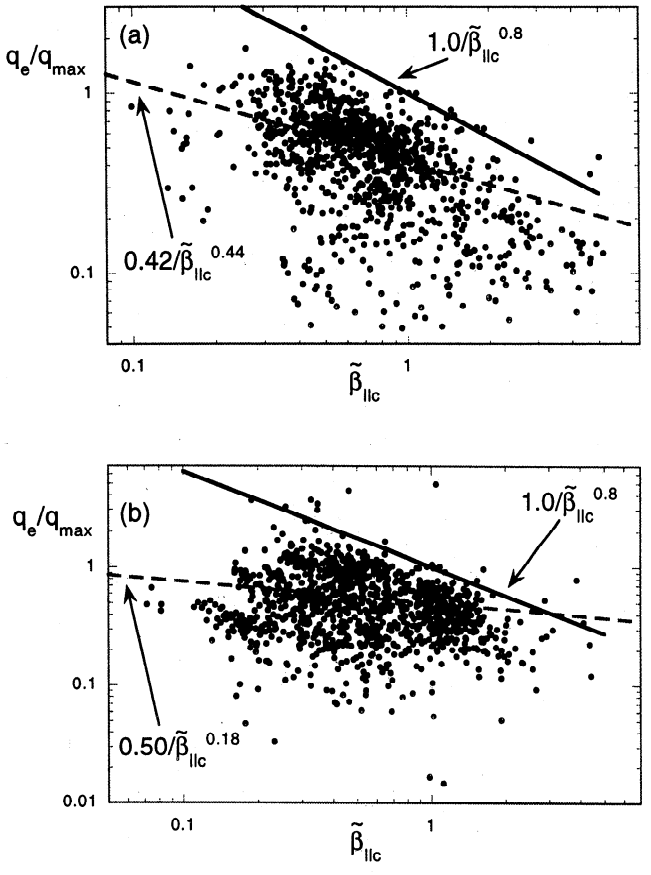

Figure 2. Dimensionless electron heat fluxes as a function of $\tilde{\beta}_{\|c}$ from the three-dimensional integrated and rotated Ulysses data set represented as individual dots. Here $q_e/q_{\max}$ is shown over (a) $1.6 \leq R < 2.0$ and (b) $3.6 \leq R < 4.0$. The dashed lines represent least squares fits to the data using power laws of $\tilde{\beta}_{\|c}$. The solid lines represents the average threshold condition for the whistler heat flux instability at $\gamma_m/\Omega_p = 0.01$ expressed as equation (2) with the fitting parameters of equation (3).

with an effective slope similar to that of the threshold. Thus we conclude that this average threshold condition provides a statistical upper bound for the observed dimensionless heat flux.

Although there are a significant number of dimensionless heat flux values clustered just below the threshold condition in Figures 1e, 2a, and 2b, there are a larger number of points distributed well below the solid lines in these same figures. Our interpretation of this result, which is observed for the other six radial bins considered here as well as for the $q_e/q_{\max}$ versus $\tilde{\beta}_{\|c}$ plot near $R = 1.4$ of *Gary et al.* [1999], is that under nominal conditions the solar wind is stable to the whistler heat flux instability. Changes in the large scale conditions of the medium induce sporadic, comparatively brief enhancements of the heat flux up to the value at which the instability is excited. At this point wave-particle scattering is enhanced, and the upper bound on $q_e/q_{\max}$ is imposed, leading to a clustering of dimensionless heat flux values at or just below the instability threshold condition. Subsequent scattering by the weaker field fluctuations during nominal conditions will slowly reduce the heat flux to values well below the threshold until the next sporadic increase in q_e. This picture, which qualitatively accounts for the observations of relatively broad distributions of $q_e/q_{\max}$, is also consistent with time series observations in the solar wind which show sporadic bursts of enhanced q_e [*Scime et al.*, 1994b], which are often correlated with bursts of enhanced whistler-like magnetic field fluctuations [*Lin et al.*, 1998].

It is more difficult to interpret the relatively few points which lie well above the threshold condition in the $q_e/q_{\max}$ versus $\tilde{\beta}_{\|c}$ plots. They may represent single-point fluctuations in either the solar wind or the measurement process, in which case they are not statistically significant. On the other hand, there is a weak correlation between the most outlying of these points and high halo temperatures ($T_{\|h}/T_{\|c} > 30$), suggesting that they may represent a non-Maxwellian property of the halo (such as an enhanced strahl) which violates the assumptions of our theory and thereby permits heat fluxes which exceed our predicted upper bound. This is certainly a subject worthy of study but is beyond the purview of the present manuscript.

Gary et al. [1998] hypothesized that the critical value of $\tilde{\beta}_{\|c}$ for the whistler heat flux instability corresponds to a lower bound on this parameter. To test this hypothesis, we plotted histograms of the observed values of $\log(\tilde{\beta}_{\|c})$ in each radial bin, calculated the mean and the standard deviation σ in each bin, and then determined the $\tilde{\beta}_{\|c}$ corresponding to 2σ below the mean of each distribution. The results, which are an approximate lower bound for $\tilde{\beta}_{\|c}$ in each bin, are plotted as dots in Figure 3. The error bars represent values of $\tilde{\beta}_{\|c}$ corresponding to σ and 3σ on the $\log(\tilde{\beta}_{\|c})$ distributions. The dashed line in this figure represents the linear theory result of (4) for comparison. The scatter in the data is too large to draw quantitative conclusions; however, we can say that observations and theory are not inconsistent. Further tests of this hypothesis, with better statistics for the data, are necessary.

6. Conclusions

Linear theory predicts that the threshold condition for the whistler heat flux instability may assume the form of

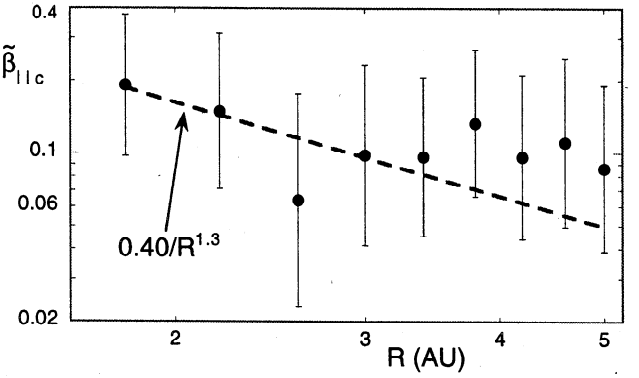

Figure 3. Comparison of Ulysses observations and linear theory. The dots and error bars represent the experimental determination of the lower bound on $\tilde{\beta}_{\|c}$ as described in the text. The dashed line represents the critical $\tilde{\beta}_{\|c}$ value of the whistler heat flux instability at $\gamma_m/\Omega_p = 0.10$ as determined from linear theory, equation (4).

(2). *Gary et al.* [1994] proposed that this threshold should correspond to an observable upper bound on the electron heat flux in the solar wind. To test this proposal, we carried out statistical analyses of dimensionless electron parameters observed from the initial in-ecliptic phase of the Ulysses mission. We used these observational results to cast the average threshold condition of the whistler instability as a concise function of $\tilde{\beta}_{\|c}$. Our comparison of theory and observations shows that solar wind heat flux observations are statistically constrained by this condition, thereby substantiating the proposal of *Gary et al.* [1994].

This result, derived from local considerations, is consistent with the conclusion which *Scime et al.* [1994b] reached from a global analysis; that is, the whistler heat flux instability makes a significant contribution to the observed reduction in the solar wind heat flux. Therefore we recommend that an upper bound of the form of (2) with fitting parameters given by (3) should be applied on the domain $0.10 \leq \tilde{\beta}_{\|c} \leq 5.0$ to all models of the collisionless solar wind which include electron thermal transport [*Scime et al.*, 1994b; *Mikić et al.*, 1999]. We hypothesize that this expression also may describe the electron heat flux constraint in many stellar winds and other collisionless astrophysical plasmas with the same domain of β_e [*Pistinner and Eichler*, 1998].

Linear theory also predicts that there is a critical value of $\tilde{\beta}_{\|c}$ below which the whistler heat flux instability does not have appreciable growth. *Gary et al.* [1998] hypothesized that this critical value corresponds to a lower bound on the values of this parameter observed in the solar wind. Our comparison of linear theory and observations yields results which are not inconsistent with this hypothesis, but a stronger test of this idea will require a data set with better statistics.

Further tests of these two proposals should involve not only more extensive data analysis but also computer simulations. It is simulations which have the potential to tie together linear theory and observations into a consistent picture for electron heat flux dissipation and core heating in the solar wind.

Appendix: Definitions

We use subscripts $\|$ and $\perp$ to denote directions relative to $\mathbf{B}_o$, the background magnetic field. The subscript p denotes protons, e corresponds to quantities representing overall electron properties, for example, $n_e = n_c + n_h$, and n_i represents the total ion density, i.e., $n_i = n_p + 2n_\alpha$. A useful dimensionless measure of the temperature of the jth component is $\tilde{\beta}_{\|j} \equiv 8\pi n_p k_B T_{\|j}/B_o^2$. We also define the cyclotron frequency of the jth species, $\Omega_j \equiv e_j B_o/m_j c$, the thermal speed of the jth species or component, $v_j \equiv \sqrt{k_B T_{\|j}/m_j}$, and the Alfvén speed $v_A \equiv B_o/\sqrt{4\pi n_i m_p}$.

The average drift velocity of the jth component parallel to $\mathbf{B}_o$ is denoted by $\mathbf{v}_{oj}$, and the relative core/halo average drift velocity is $\mathbf{v}_o = \mathbf{v}_{oc} - \mathbf{v}_{oh}$. If both the halo and core are described in terms of drifting bi-Maxwellian distributions, the heat flux is

$$q_e = \frac{m_e}{2} \sum_{j=c,h} n_j v_{oj} \left[\left(3 + 2\frac{T_{\perp j}}{T_{\|j}} \right) v_j^2 + v_{oj}^2 \right] .$$

We define the heat flux normalization factor as $q_{\max} \equiv 3 m_e n_i v_c^3/2$.

Acknowledgments. We acknowledge useful discussions with Bill Feldman and Dave McComas, and support from Ed Santiago and Michelle Thomsen. The work at Los Alamos was performed under the auspices of the U.S. Department of Energy (DOE) and was supported in part by the DOE Office of Basic Energy Sciences, Division of Engineering and Geosciences, the Laboratory Directed Research and Development program at Los Alamos, and the NASA Ulysses Program. The research conducted at the Jet Propulsion Laboratory, California Institute of Technology, was performed under contract to the National Aeronautics and Space Administration.

Janet G. Luhmann thanks Keith W. Ogilvie and another referee for their assistance in evaluating this paper.

References

Abraham-Shrauner, B., and W. C. Feldman, Whistler heat flux instability in the solar wind with bi-Lorentzian velocity distribution functions, *J. Geophys. Res.*, *82*, 1889, 1977.

Bame, S. J., D. J. McComas, B. L. Barraclough, J. L. Phillips, K. J. Sofaly, J. C. Chavez, B. E. Goldstein, and R. K. Sakurai, The Ulysses solar wind plasma experiment, *Astron. Astrophys. Suppl. Ser.*, *92*, 221, 1992.

Feldman, W. C., J. R. Asbridge, S. J. Bame, M. D. Montgomery, and S. P. Gary, Solar wind electrons, *J. Geophys. Res.*, *80*, 4181, 1975.

Feldman, W. C., J. R. Asbridge, S. J. Bame, S. P. Gary, and M. D. Montgomery, Electron parameter correlations in high-speed streams and heat flux instabilities, *J. Geophys. Res.*, *81*, 2377, 1976a.

Feldman, W. C., J. R. Asbridge, S. J. Bame, S. P. Gary, M. D. Montgomery, and S. M. Zink, Evidence for the regulation of solar wind heat flux at 1 AU, *J. Geophys. Res.*, *81*, 5207, 1976b.

Feldman, W. C., B. L. Barraclough, J. T. Gosling, D. J. McComas, P. Riley, B. E. Goldstein, and A. Balogh, Ion energy equation for the high-speed solar wind: Ulysses observations, *J. Geophys. Res.*, *103*, 14,547, 1998.

Fitzenreiter, R. J., K. W. Ogilvie, D. J. Chornay, and J. Keller, Observations of electron velocity distribution functions in the solar wind by the WIND spacecraft: High angular resolution strahl measurements, *Geophys. Res. Lett.*, *25*, 249, 1998.

Gary, S. P., Ion-acoustic-like instabilities in the solar wind, *J. Geophys. Res.*, *83*, 2504, 1978.

Gary, S. P., and J. Wang, Whistler instability: Electron anisotropy upper bound, *J. Geophys. Res.*, *101*, 10,749, 1996.

Gary, S. P., W. C. Feldman, D. W. Forslund, and M. D. Montgomery, Electron heat flux instabilities in the solar wind, *Geophys. Res. Lett.*, *2*, 79, 1975a.

Gary, S. P., W. C. Feldman, D. W. Forslund, and M. D. Montgomery, Heat flux instabilities in the solar wind, *J. Geophys. Res.*, *80*, 4197, 1975b.

Gary, S. P., E. E. Scime, J. L. Phillips, and W. C. Feldman, The whistler heat flux instability: Threshold conditions in the solar wind, *J. Geophys. Res.*, *99*, 23,391, 1994.

Gary, S. P., M. F. Thomsen, L. Yin, and D. Winske, Electromagnetic proton cyclotron instability: Interactions with magnetospheric protons, *J. Geophys. Res.*, *100*, 21,961, 1995.

Gary, S. P., J. Wang, D. Winske, and S. A. Fuselier, Proton temperature anisotropy upper bound, *J. Geophys. Res.*, *102*, 27,159, 1997.

Gary, S. P., J. A. Newbury, and B. E. Goldstein, Lower bound for electron core beta in the solar wind, *J. Geophys. Res.*, *103*, 14,559, 1998.

Gary, S. P., R. M. Skoug, and W. Daughton, Electron heat flux constraints in the solar wind, *Phys. Plasmas*, *6*, 2607, 1999.

Lengyel-Frey, D., R. A. Hess, R. J. MacDowall, R. G. Stone, N. Lin, A. Balogh, and R. Forsyth, Ulysses observations of whistler waves at interplanetary shocks and in the solar wind, *J. Geophys. Res.*, *101*, 27,555, 1996.

Lin, N., P. J. Kellogg, R. J. MacDowall, E. E. Scime, A. Balogh, R. J. Forsyth, D. J. McComas, and J. L. Phillips, Very low frequency waves in the heliosphere: Ulysses observations, *J. Geophys. Res.*, *103*, 12,023, 1998.

Maksimovic, M., V. Pierrard, and P. Riley, Ulysses electron distributions fitted with Kappa functions, *Geophys. Res. Lett.*, *24*, 1151, 1997.

Marsch, E., Kinetic physics of the solar wind plasma, in *Physics of the Inner Heliosphere, II, Particles, Waves and Turbulence*, edited by R. Schwenn and E. Marsch, pp. 45-133, Springer-Verlag, New York, 1991.

Meyer-Vernet, N., and K. Issautier, Electron temperature in the solar wind: Generic radial variation from kinetic collisionless models, *J. Geophys. Res.*, *103*, 29,705, 1998.

Mikić, Z., J. A. Linker, D. D. Schnack, R. Lionello, and A. Tarditi, Magnetohydrodynamic modeling of the global solar corona, *Phys. Plasmas*, *6*, 2217, 1999.

Newbury, J. A., C. T. Russell, J. L. Phillips, and S. P. Gary, Electron temperature in the ambient solar wind: Typical properties and a lower bound at 1 AU, *J. Geophys. Res.*, *103*, 9553, 1998.

Phillips, J. L., S. J. Bame, S. P. Gary, J. T. Gosling, E. E. Scime, and R. J. Forsyth, Radial and meridional trends in solar wind thermal electron temperature and anisotropy: Ulysses, *Space Sci. Rev.*, *72*, 109, 1995.

Pilipp, W. G., H. Miggenrieder, K.-H. Mühlhäuser, H. Rosenbauer, and R. Schwenn, Large-scale variations of thermal electron parameters in the solar wind between 0.3 and 1 AU, *J. Geophys. Res.*, *95*, 6305, 1990.

Pistinner, S. L., and D. Eichler, Self-inhibiting heat flux, *Mon. Not. R. Astron. Soc.*, *301*, 49, 1998.

Scime, E. E., J. L. Phillips, and S. J. Bame, Effects of spacecraft potential on three-dimensional electron measurements in the solar wind, *J. Geophys. Res.*, *99*, 14,769, 1994a.

Scime, E. E., S. J. Bame, W. C. Feldman, S. P. Gary, and J. L. Phillips, Regulation of the solar wind electron heat flux from 1 to 5 AU: Ulysses observations, *J. Geophys. Res.*, *99*, 23,401, 1994b.

S. P. Gary, E. Neagu, and R. M. Skoug, M.S. D466, Los Alamos National Laboratory, Los Alamos, NM 87545. (pgary@lanl.gov; url: htpp://nis-www.lanl.gov/~pgary/; eneagu@lanl.gov; rskoug@lanl.gov)

B. E. Goldstein, Jet Propulsion Laboratory, MS 169-506, 4800 Oak Grove Drive, Pasadena, CA 91109. (bgoldstein@jplsp.jpl.nasa.gov)

(Received January 8, 1999; revised May 18, 1999; accepted June 1, 1999.)